Artificial Intelligence Algorithms for Rapeseed Fields Mapping Using Sentinel-1 Time Series: Temporal Transfer Scenario and Ground Sampling Constraints

Saeideh Maleki, Nicolas Baghdadi, Cassio Fraga Dantas, Sami Najem, Hassan Bazzi, Núria Pantaleoni Reluy, Dino Ienco, and Mehrez Zribi

***Abstract*—This study aims to enhance rapeseed field detection accuracy using Sentinel-1 (S1) time series data and addressing challenges in collecting ground samples. The proposed solutions include model transfer between years without retraining and secondly, developing models with limited training samples. The research evaluates the performance of Random Forest (RF) and three deep learning (DL) algorithms: Long Short-Term Memory Fully Convolutional Network (LSTM-FCN), InceptionTime, and Multi-layer Perceptron (MLP). All four algorithms are evaluated initially with abundant ground samples and later with smaller sample sizes (100, 300, 500 and 1000 samples). Model transferability is tested across years. The impact of S1 image count on transfer accuracy is examined. Additionally, the effect of the phenological shift in the rapeseed growth cycle of 15 and 30 days between the training and test years was also investigated. The findings demonstrate strong model performance when training and testing occur in the same year (F1-score up to 95%). Within sample sizes of 300 to 1000, RF and InceptionTime stand out with high accuracy (F1-score>90%). When employing different years for training and testing with abundant sample sizes, all four algorithms correctly classified rapeseed (F1-score between 85.5% and 92.7%). In cases of a reduced number of images, the performance of InceptionTime and LSTM-FCN decreased (16% decrease in the F1-score), while RF and MLP maintain their performance. Notably, RF outperforms DL algorithms with an F1-score of 89.1%. In the context of a phenological shift, only InceptionTime and LSTM-FCN demonstrated strong performance (F1-score between 87.7% and 92.6%).**

***Index Terms*—Deep learning (DL), INCEPTIONTIME, long short-term memory fully convolutional network (LSTM-FCN), multilayer perceptron (MLP), random forest (RF), rapeseed, sentinel-1, temporal transferability.**

Manuscript received 6 May 2023; revised 16 July 2023 and 16 August 2023; accepted 6 September 2023. Date of publication 18 September 2023; date of current version 2 October 2023. This work was supported in part by the French Space Study Center (CNES, TOSCA 2023) and in part by the National Research Institute for Agriculture, Food and the Environment. *(Corresponding author: Saeideh Maleki.)*

Saeideh Maleki, Nicolas Baghdadi, Cassio Fraga Dantas, Sami Najem, Núria Pantaleoni Reluy, and Dino Ienco are with the TETIS, Université de Montpellier, CIRAD/CNRS/INRAE, 34093 Montpellier, France (e-mail: saeideh.maleki-najafabadi@inrae.fr; nicolas.baghdadi@inrae.fr; cassio.fraga-dantas@inrae.fr; sami.najem@inrae.fr; nuria.pantaleoni@upc.edu; dino.ienco@inrae.fr).

Hassan Bazzi is with the Atos France, Technical Services, 95870 Bezons, France (e-mail: hassan.bazzi@atos.net).

Mehrez Zribi is with the CESBIO, Université de Toulouse, CNES/CNRS/INRAE/IRD/UPS, 31401 Toulouse, France (e-mail: mehrez.zribi@ird.fr).

Digital Object Identifier 10.1109/JSTARS.2023.3316304

I. Introduction

THE aftermath of the COVID-19 pandemic and the war in Ukraine have exacerbated threats to global food security [1]. To avert this threat, the global community needs to expand the cultivation of key crops and improve agricultural efficiency, especially for multipurpose crops such as rapeseed, which is important not only for food security but also for oil and livestock production [2]. Based on the United States Department of Agriculture report on rapeseed production by country in 2022, the top 7 rapeseed producers in the world are the European Union, Canada, China, India, Australia, Ukraine, and Russia [3]. Therefore, accurate information about the expansion of the rapeseed cultivation is important, not only for agricultural planning, but also for environmental and economic purposes [4].

Satellite imagery with different spatial, spectral, and temporal resolutions facilitates the provision of crop information [5], [6]. However, using optical data, previous studies mentioned several challenges in detecting rapeseed, such as the similarity between the spectral response of some rapeseed phenological stages and other vegetation species, spectral mixing pixels of moderate resolution images, cloud contamination, and limitations in achieving training samples in extensive farms [7], [8]. To address these limitations, different methods and types of satellite imagery have been used so far. Phenology-based classification methods are mainly based on the difference between the growth stages of rapeseed and other crops [9]. For example, the yellow color of rapeseed during the flowering stage has been widely used to detect rapeseed [2], [8], [10]. The normalized difference yellow index is known to be an effective index for mapping rapeseed using optical images [5], [8], [10]. In addition, the ratio oilseed rape colorimetric index and the normalized rapeseed flowering index were developed respectively by Wang et al. [11] and Han et al. [10], based on the yellow color of rapeseed flowers.

In the vast regions, where rapeseed planting dates vary, the availability of continuous time series images, covering all growth stages of rapeseed in all parts of the study area is crucial. The acquisition of optical images for the monitoring of rapeseed fields can be difficult in some regions given that this crop is a winter crop [12] and cultivated in countries with a prevalence of cloudy days [5]. Thus, synthetic aperture radar (SAR) is a good alternative, providing enough image frequency with the advantage of nondependency on weather conditions. Previous

studies have confirmed the variation in the SAR backscatter signal following the phenological changes of rapeseed [10], [13], [14]. McNairn et al. [15] described how the accumulation of biomass and changes in the structure of rapeseed during the growth stages increase the SAR backscatter. This change in the SAR backscattering over rapeseed fields with biomass accumulation has also been reported in studies of Wisemann et al. [16], Yang et al. [17], and Lopes-Sanchez et al. [18]. In addition, unlike other crops, the random shape of rapeseed leads to a higher contribution of the rapeseed plant to the SAR backscatter than that of the soil [12]. Using SAR data, the potential of VH and VV/VH to detect the peak flowering period of rapeseed is also mentioned by Han et al. [10]. In addition, Fieuzal et al. [14] showed that the best results are achieved using the C-band rather than X and L bands. Sentinel-1 (S1) C-band SAR sensors have made crop mapping easier, thanks to their high spatial and temporal resolutions and their availability in free and open access. S1 imagery provides weather-independent data with a short revisit time (up to 6 days in Europe), which has made S1 images advantageous for crop growth studies. Because of these advantages, several studies have been carried out on rapeseed mapping using SAR imagery or using a combination of the optical and SAR images [2], [4], [10], [14], [19], [20], [21], [22].

Although rapeseed mapping has been the subject of several studies, some other research arguments should be addressed, including the constraints of collecting ground samples of rapeseed fields every year due to temporal and financial constraints, the effect of the ground sample size on the accuracy of the classification, and the possibility to use a model developed using ground samples from one year on other years. This article will reply to these concerns with the advantage of artificial intelligence (AI) methods as AI exhibits a high potential to compensate for the weaknesses of classical methods [23], [24]. The ability to learn from complex and large data sources allows AI methods to map multiple crop types from multitemporal images over a large and diverse region [9], [24], [25]. In addition, the ability of AI methods to determine the importance of inputs in classification has made them more functional in time series analysis. From the various AI methods, machine learning techniques such as random forest (RF) are commonly used in crop mapping [4], [26], [27], [28]. Using a RF algorithm, Liu and Zhang [5] simulated the peak flowering date of rapeseed and Meng et al. [29] determined the best temporal period for rapeseed detection. However, deep learning (DL) methods are gaining interest in satellite image classification [23], [30], [31], [32], [33]. These methods are able to learn in an end-to-end manner from the raw input data to perform image classification [30], [34]. The DL algorithms for remote sensing data are grouped as convolutional neural networks (CNNs) for spatial learning and recurrent neural networks (RNNs) for sequential data, such as time series [23]. To improve the vanishing gradient problem of RNNs, long short-term memory (LSTM) networks using a forget gate have been developed. Recently, methods incorporating CNNs and LSTMs, such as convolutional LSTM, have been applied to remote sensing applications involving both spatial and temporal terms [35].

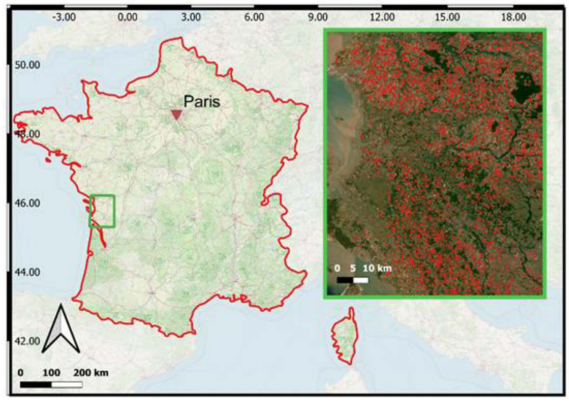

Fig. 1. Location of the study site and an example of the distribution of rapeseed plots within the study site.

In this article, the advantage of four AI algorithms, including RF, LSTM fully convolutional network (LSTM-FCN), InceptionTime, and multilayer perceptron (MLP), have been tested to facilitate the detection of rapeseed fields firstly by presenting algorithms that provide high accuracy rapeseed classification using only S1 time series. Second, by developing different solutions for mapping the rapeseed fields when there are constraints on ground sampling, by using a model trained with ground samples from one year and then applying it to other years without having to retrain it, and by testing the use of small training sample size in the classification. Also, the effect of the phenological shift in the rapeseed growth cycle between the training and test years, and the effect of the number of images in the S1 time series on the accuracy of the transferability of models were investigated. The approaches proposed in this article could enable users to detect the rapeseed fields regardless of the inaccessibility of the study site and to obtain the accurate classification of rapeseed over large regions. This paper is organized into six sections: introduction, study site and dataset, methods, results, discussion, and conclusions.

II. Study Area and Dataset

A. Study Area

This study was carried out in the Charente-Maritime department in the west of France. The study area with a geographical extent of approximately 8000 km^2 is presented in Fig. 1. It belongs to the oceanic climate zone, with about 1000 mm of rainfall and 2000 h of sunshine per year. The main crops grown in the area are wheat, maize, and sunflower. Table I shows the nine most abundant crops in the study area in the years 2018, 2019, and 2020, based on the French registry for agricultural plots (RPG, Registre Parcellaire Graphique). For each year, the proportion of each crop type relative to the total cultivated area in the study site is also provided.

B. Dataset

1) Ground Data: The ground samples were taken from the RPG data which is the database of the farmers' declarations of

TABLE I
PROPORTION OF THE CULTIVATED AREA BY THE MAIN CROPS OUT OF THE TOTAL CULTIVATED AREA IN THE STUDY SITE FOR THE YEARS 2018, 2019, AND 2020

Crop type	2018 Area (%)	2019 Area (%)	2020 Area (%)
Soft winter wheat	21.6	23.0	15.1
Maize	12.4	13.2	14.4
Permanent prairie	10.8	10.8	11.2
Sunflower	9.0	9.4	10.8
Winter rapeseed	6.0	2.0	6.2
Hard winter wheat	6.2	4.3	4.0
Peas	2.4	2.4	3.2
Winter barley	4.3	4.8	3.1
Spring Barley	2.8	4.1	2.8

TABLE II
DATASET USED IN THIS STUDY

Year	Total number of plots	Total number of Rapeseed plots	Ratio of rapeseed plots in samples	Total number of orbits	Total number of images	Number of images per month
2018	80288	2639	3.29%	3	181	15
2019	72506	1021	1.41%	3	163	14
2020	97971	1519	1.55%	3	179	15

agricultural plots in France. It contains the boundaries of each declared agricultural plot and information such as the crop type and the size of each plot. The RPG is available for download for the whole of France via.[1] To map the rapeseed fields in the current paper, the RPG data of the study years including 2018, 2019, and 2020 were used in order to create the large annual sample dataset for the training and testing. The cultivation period of rapeseed in the study area starts from September and ends in July of the next year. Therefore, for a growing season that starts from a sowing date in September 2018 and an end with a harvesting date in July 2019, the RPG of 2019 was used as the ground sample because the year of harvest is taken into account in the RPG. Table II shows the total number of cultivated plots, the number of rapeseed plots, and the proportion of rapeseed plots in the total number of cultivated plots.

2) SAR Images: The time series of C-band (5.405 GHz) SAR images acquired by the Sentinel 1A (S1A) and Sentinel 1B (S1B) satellites were used. Both "ascending" (evening at 18:00 UT) and "descending" (morning at 06:00 UT) acquisitions were utilized in the VV and the VH polarizations. The pixel spacing of S1 images is 10 m x 10 m. The data are freely available from the European Space Agency's (ESA) website (https://scihub.copernicus.eu/dhus/#/home). The revisit time of the S1 constellation is six days, meaning that one image is available for each orbit every six days. In this study, a dataset of all available orbits over the study area was collected. All the acquired images regardless of the orbit number were stacked in chronological order. Table II shows the total number of S1 images acquired over the study site and the average number of images per month.

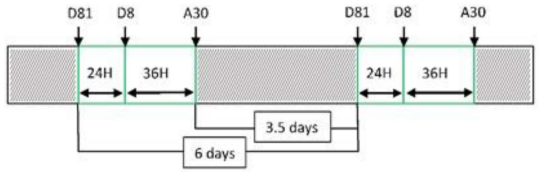

Fig. 2. Frequency of S1 images in "ascending" (a) and "descending" (d) for all orbits covering our study site. The hatched area represents the period with no S1 acquisitions.

Fig. 2 shows the temporal distribution and the overall coverage of the S1 orbits over the study site (each orbit has a unique acquisition time). The first acquisition in our study site is a "descending" image belonging to the orbit 81 (D81). The following image comes 24 h later and is a descending acquisition as well from orbit 8 (D8). Then, the third acquisition comes 36 h later as an ascending acquisition from orbit 30 (A30). Six days after the first image, the cycle is repeated in the same way with a new image from D81 orbit. The hatched area in Fig. 2 represents the 3.5 days period that separates every bunch of three images (D81, D8, A30) from the next bunch. The incidence angles vary on our study site from 23° to 38° for the orbit 81 and from 32° to 48° for the two orbits 8 and 30.

The S1 images were calibrated using the S1 toolbox developed by ESA. Calibration was a two-step process; the first step was the radiometric calibration, which converted a digital number into a backscatter coefficient σ° in linear units. The second step was the geometric correction, which was the process of ortho-rectifying the images using a 30 m digital elevation model from the shuttle radar topography mission.

For our dataset, which covers an area of 100 km x 100 km, the incidence angle varies by about 15°. In order to reduce the effect of the incidence angle, a possible solution would have been to normalize its effect. However, the normalization function can be different from one crop to another but also different for the same crop between the different parts of the growth cycle (bare soil, well-developed vegetation, etc.). Furthermore, it is not well known for each specific type of crop. When using a normalization function of the form $\cos(\theta)$ [36] and a reference incidence angle of 35°, the variation in the radar signal due to the difference in the incidence angle is lower than 1 dB (our dataset acquired with incidence angles between 23° and 48°). As the form of the normalization function is not well known and the variation of radar signal due to the incidence angle is smaller than the increase of the signal due to vegetation growth (several dB), we did not normalize by the radar incidence angle, thus leaving the rapeseed mapping algorithms to overcome small fluctuations in the radar signal due to a variation in the incidence angle.

3) Sentinel-2 Images (S2): Sentinel2 images were downloaded from the Theia website.[2] These images were used to calculate the NDVI values with the goal to only explain and interpret the temporal behavior of the S1 signals over rapeseed

[1][Online]. Available: https://www.data.gouv.fr/en/datasets/registre-parcellaire-graphique-rpg-contours-des-parcelles-et-ilots-culturaux-et-leur-groupe-de-cultures-majoritaire/

[2][Online]. Avilable: https://www.theia-land.fr/

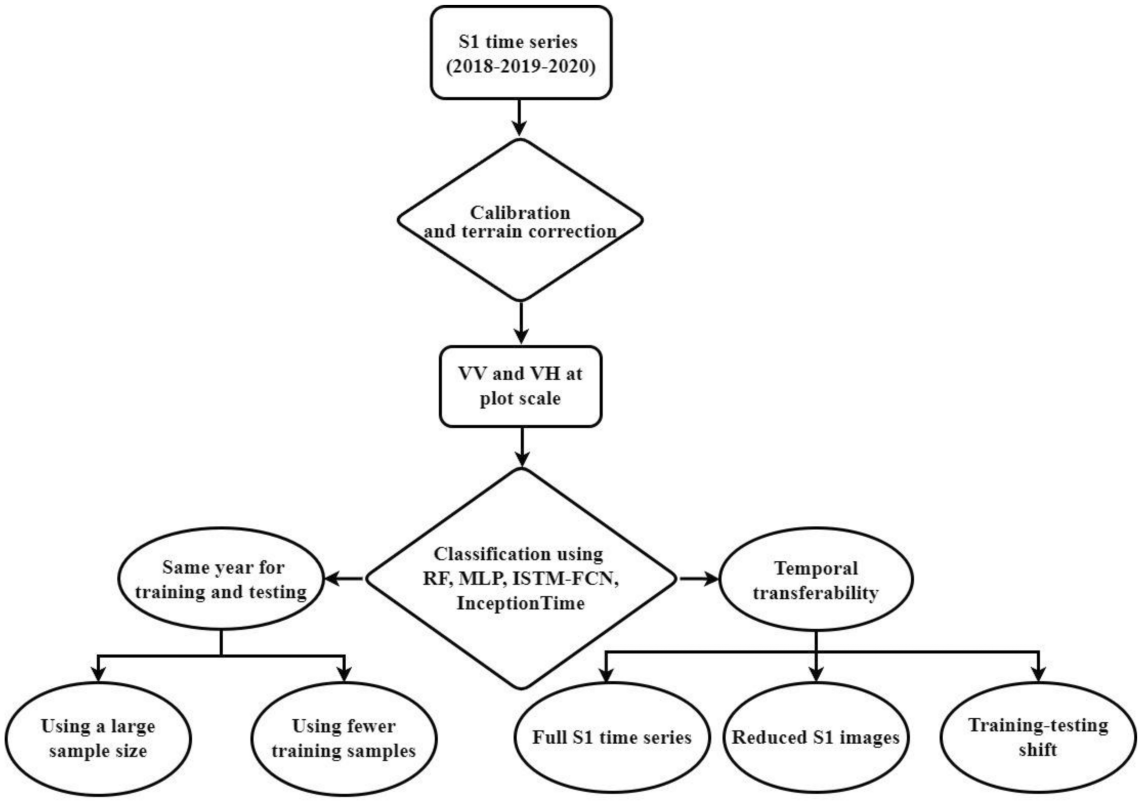

Fig. 3. Flowchart of method.

fields. Thus, optical related information was not involved in the classification process.

III. Method

A. Temporal Behavior of Sentinel-1 Signals

The temporal behavior of S1 over rapeseed fields was studied for the 2018, 2019, and 2020 growing seasons (the growing season starts in September and ends in July of the following year). For this study, an S1 dataset consisting of all three orbits (8, 30, 81) available over the study area was used. Since this work was conducted at plot scale, the average signal of all pixels in each plot was calculated to obtain a single representative value for each plot. The result of this process was two plot level time series (marked with a "p"), VVp and VHp.

B. Rapeseed Fields Mapping

With the aim of evaluating the ability of AI algorithms for rapeseed fields mapping and proposing an algorithm to overcome some functional constraints in land cover classification, four AI algorithms were evaluated. One machine learning and three DL algorithms were used to detect the rapeseed fields from S1 time series. The flowchart of the methodology of this article is presented in Fig. 3, and the codes are available at GitHub.[3] Within the machine learning methods, RF was selected as a well-known method widely used in similar land cover classification approaches and providing acceptable classification results [28], [37], [38]. RF was used in this study as a baseline for accuracy of classification by different algorithms. Within the DL methods, MLP, which is a plain deep artificial neural networks (ANNs), and two ANNs algorithms tailored for time series analysis called LSTM-FCN [39] and InceptionTime [40] were selected. A more detailed description of the selected algorithms is provided in Section C of methodology. The Adam optimizer was used to train all three DL algorithms [25]. Parameters of Adam were fixed as: $\beta 1 = 0.9$, $\beta 2 = 0.999$, $\varepsilon =$ 1e–07. The learning rate and weight decay were set respectively as 1e–5 and 1e–6. The batch size was set to 16 during training and a standard cross-entropy loss function was used. The input data were the S1 time series in two channels at plot scale (VHp and VVp) covering three years (2018, 2019, and 2020). The classification process was performed with the aim of detecting the rapeseed fields, so two classes were used: rapeseed (positive class) and nonrapeseed (negative class). Nonrapeseed class consisted of other crops except rapeseed. Each classification was performed with 70% of the ground samples as training and 30% as test data, split randomly in five independent realizations. The classification was carried out in two main parts including rapeseed fields mapping using the same year for training and testing, and evaluating the transferability of the models obtained by each algorithm in each year onto other years. In each part, related factors that might affect the accuracy of the mapping were tested.

1) Rapeseed Fields Mapping Using the Same Year for Training and Testing: Rapeseed fields mapping using the same year

[3][Online]. Available: https://github.com/cassiofragadantas/Colza_Classif

for training and for testing was conducted using all four algorithms. To train the algorithms and test the models all ground samples mentioned in Table II (large annual sample dataset) were employed.

2) Rapeseed Fields Mapping Using Smaller Training Sample Size: The effect of the training sample size on the performance of the four algorithms in the detection of rapeseed fields was evaluated using the same year for training and for testing and four different sample sizes including 100, 300, 500, and 1000 samples. The input time series were VV and VH time series at plot scale (VHp and VVp). The training samples were drawn by keeping the same ratio between positive and negative classes as found in the large annual sample dataset (imbalanced training data). For example, in the large dataset of the year 2018, the percentage of rapeseed and nonrapeseed samples was about 3% and 97%, respectively. Therefore, with a training sample size of 1000, the number of rapeseeds fields in the training samples was around 30 and the number of nonrapeseed fields was around 970.

3) Transferability of the Models Using Different Years for Training and Testing: The transferability of models was investigated by training the four algorithms using samples from one year and deploying the models on the other years. The large annual sample dataset shown in Table II was used as the base sample dataset. The transferability was investigated using six combinations of training and test data, including training using the samples of 2018 and testing with the samples of 2019 and 2020, training using the samples of 2019 and testing with the samples of 2018 and 2020, and training using the samples of 2020 and testing by the samples of 2018 and 2019.

4) Effect of the Number of Images and the Shift in the Phenological Cycle Between the Training and Test Years on the Transferability of the Models:

a) Transferability of the models using a reduced number of S1 images (only one orbit): To investigate the effect of the number of S1 images in the time series (i.e., the time resolution), the transferability analysis described in Section III-B3 of methodology was repeated using only S1 data of a single orbit (orbit 8) for the six training-test years' combinations. The large annual sample dataset presented in Table II was used as ground samples.

b) Transferability of the models with a shift in the phenological cycle between training and test years: The phenological cycle of rapeseed can be different between two years on the same site if, for example, the climatic conditions (mainly temperature and rainfall) are different [22], [41]. This phenomenon could be observed more frequently due to climate change. This difference in the phenological cycle can also be observed between two different sites [41], [42]. The difference between sites and years could cause both the temporal shift and the difference in the duration of the growing cycle of rapeseed. In this article, only the temporal shift in the phenological cycle between training and test years has been investigated by considering the case of a shift of 15 days and another of 30 days. The shift in the phenological stages of crops over years (also over regions) could affect the accuracy of mapping using different years as training and test. This is important because, even between sites with similar climatic conditions (e.g., in Europe and even in France), sowing and harvesting of rapeseed take place at within +/- 1 month [43]. The transferability test of the models that were developed in Section III-B3 of methodology was also carried out on the cases where the growth stages of rapeseed between the training year and test years do not align perfectly. The phenological shift in the growth stage of rapeseed was simulated in dataset of 2018, considered as the training year. The trained algorithm with the shifted dataset of 2018 was used to classify the dataset of 2020, considered as the test year. Two periods of phenological shift were simulated by removing days from the beginning of the training time series (the whole S1 time series was thus shifted by 15 or 30 days). In order to obtain the same size for the training and test data sets, the days were removed from the last part of the test time series, which did not include the main phenological cycle of rapeseed. More precisely, after removing the days from the beginning of the training dataset, the same size for training and testing was achieved using the overlapping part of both time series. In this case, the large annual sample dataset shown in Table II was used.

5) Performance Assessment: To evaluate the results of the classification in each use case, the precision, recall and F1 were applied. Table III shows the description and equation of these accuracy metrics.

C. Algorithms

1) Random Forest: RF algorithm consists of several decision trees, where the results of trees are merged to create the final results [28], [44]. It is a meta-estimator that adapts multiple decision tree classifiers to multiple parts of the dataset, and applies the average of all parts to improve the accuracy of results and control overfitting [45]. Although RF is not sensitive to the selection of hyperparameters [37], the accuracy of the results of the RF approach is related to the number of trees. The number of trees in this study was set as 100. Other parameters were set as default.

2) Multilayer Perceptron: MLP algorithm is the DL model that has the simplest and most traditional architecture, where neurons in each layer are connected to all neurons in the neighboring layers [35], [46]. The basic component of MLP includes several nodes with weights and biases in multiple fully connected layers [25]. In the MLP algorithm, the learning approach of the weights and biases within the networks to simulate the relationship between the input features and the output features is performed in a backpropagation manner [25]. Since MLP has the simplest architecture of ANNs, it was used as a basis to evaluate the performance of other ANNs algorithms. In the MLP algorithm, the number of hidden layers and neurons are defined as hyper-parameters. Since all the hidden layers are connected in MLP, more layers lead to higher complexity [25]. In this paper, a standard MLP architecture was used with 2 hidden layers containing 256 neurons each, plus the input and output layers. A batch normalization and a rectified linear unit nonlinearity were used on the two hidden layers. Finally, a dropout rate of 0.5 was used during training.

TABLE III
DESCRIPTION AND THE EQUATION OF THE ACCURACY METRICS THAT ARE USED IN THIS STUDY

Metric	Description	Equation	Reference
Recall	Recall shows the ability of the algorithm to detect all positive cases. It shows the proportion of the positive classes in the ground samples that are detected in the results.	$\frac{TP}{TP+FN}$	[47]
Precision	Precision shows the ability of the algorithm to return the correct results. Precision aims to show the proportion of the detected positive classes in the results that are actually correct.	$\frac{TP}{TP+FP}$	[48]
F1	The weighted combination of precision and recall.	$\frac{2*(Precision*Recall)}{Precision+Recall}$	[49]

3) Long Short-Term Memory Fully Convolutional Network: LSTM-FCN is formed by adding the FCN, which take advantage of CNNs, with long short-term memory recurrent neural network, which is in the group of RNNs for time series classification [39] The methods that utilize the CNNs architecture are used for spatial learning whereas the RNNs architecture is utilized for sequential learning [23]. In the current study, one type of LSTM-FCN developed by Karim et al. [39] for multivariate time series classification was used to map rapeseed fields. In this algorithm, the squeeze and excitation block were added to the structure of the univariate model and the fully conventional blocks were increased to improve the accuracy of the results [39]. The advantage of this model is that it outperforms most state-of-the-art models with less preprocessing. The efficiency of this algorithm in analyzing complex multivariate time series classification, such as action recognition, and the possibility to deploy this algorithm on constrained systems was shown by Karim et al. [39]. The default model hyperparameters proposed by Karim et al. [39] were used in our experiments.

4) InceptionTime: The InceptionTime algorithm was introduced by Fawaz et al. [40] for multivariate time series analysis. It is a collection of five deep learning models, each consisting of two residual blocks which, in turn, contain three so-called Inception modules. The Inception modules apply multiple one-dimensional convolutional filters of different lengths to the input data, which allows the network to extract features from the time series at different scales. Because a single inception network may be subject to high deviations in its accuracy, an ensemble of networks with different weight initializations is used. Moreover, the common vanishing gradient problem for deep networks is tackled by the shortcut connections between residual blocks which allow for a direct gradient flow. When deploying this algorithm, the difference between the default and the best hyperparameters is usually not significant [40]. Therefore, in this study, the hyperparameters were set as default.

IV. RESULTS

A. Temporal Behavior of Sentinel-1 Signals

Fig. 4(a) and (b) show the mean and standard deviation (represented by shading) of the S1 backscattering coefficient in VHp and VVp polarizations over rapeseed fields during the cultivation period of 2018, 2019, and 2020. Rainfall during this period in 2020 is presented using the secondary *Y*-axis in Fig. 4(a) and (b). In this study area, the cultivation period starts from September and ends in July of the following year (see Fig. 5). High amplitude and frequent variation in S1 signal at VV and VH polarizations are observed at the plot scale [see Fig. 4(a) and (b)]. As previous studies showed [8], [12], [14] this frequent variation in S1 backscatter is mainly due to precipitation altering the soil moisture values.

The temporal behavior of both VHp and VVp polarizations shows four main phases. First, an increasing trend is seen between September and November (from –20.5 to 14 dB for VHp and from –12.5 to –7.5 dB for VVp. The values of both polarizations then remain stable between November and March. Next, the signal increases from March to reach its highest value at the beginning of June (about –10.5 dB in VHp and –6 dB in VVp). Then, both polarizations decrease from the middle of June till July where the value VHp and VVp falls below –16 and –10 dB, respectively. It is worth mentioning that the VHp shows a stronger vegetation growth dynamic than VVp with the different stages of the rapeseed phenological cycle.

B. Rapeseed Fields Mapping

1) Rapeseed Fields Mapping Using the Same Year for Training and Testing: In this section, the performance of the four considered algorithms to map the rapeseed fields in the case where the same year is used for the training and test phases was evaluated. The results of the accuracy assessment of rapeseed fields mapping using the four algorithms are shown in Table IV. Accuracy metrics are presented in this table as an average value over all three years (Mean), the maximum value of each metric within three years (Max), and the minimum value within three years (Min). The results show that all algorithms have a mean F1 close to 95%. However, InceptionTime gave the highest mean F1 values (95.7%). Moreover, smaller differences between the min and max of F1 are obtained with InceptionTime (0.3%), which shows the stability of the classification results across the years using this algorithm. In contrast, the highest differences between the min, and the max of F1 are obtained

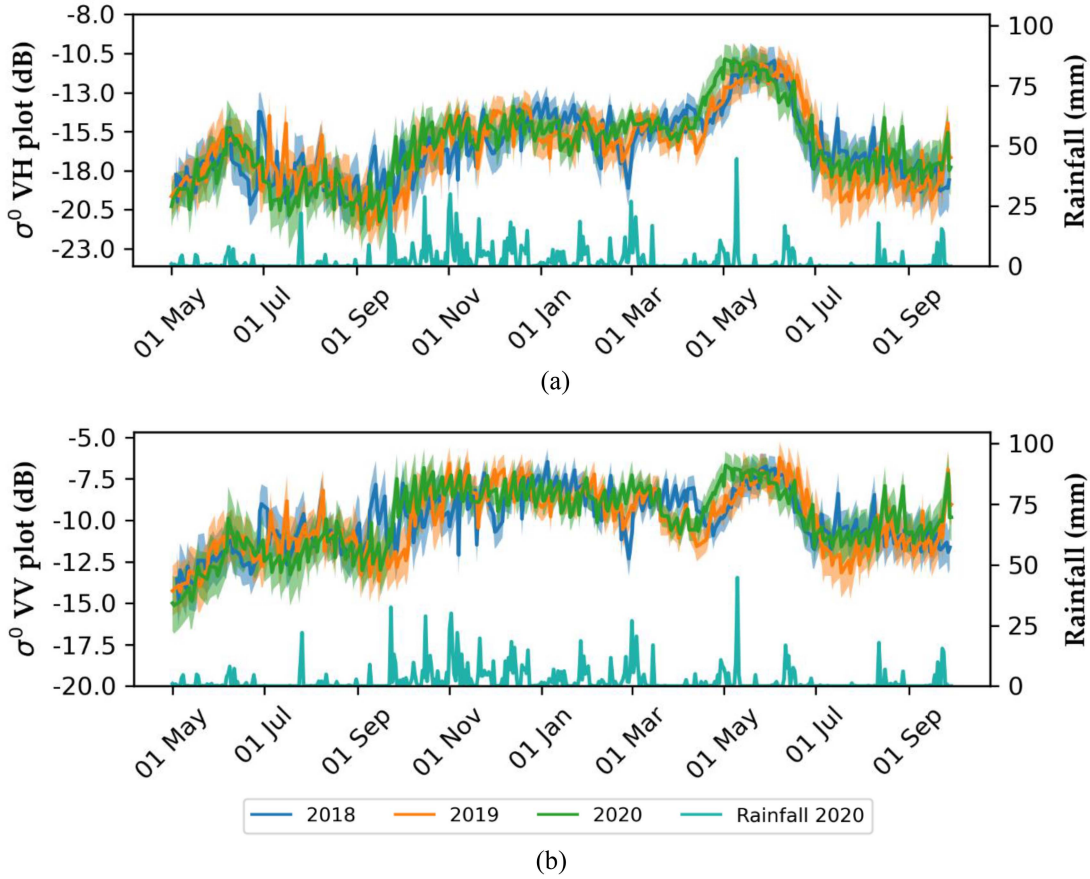

Fig. 4. Sentinel-1 temporal behavior over rapeseed fields in 2018, 2019, and 2020. (a) VH at the plot scale (VHp). (b) VV at the plot scale (VVp). The mean values are represented by bold lines and the standard deviation by the shaded areas. The rainfall events in the cultivation period of rapeseed in 2020 is presented using the secondary *Y*-axis.

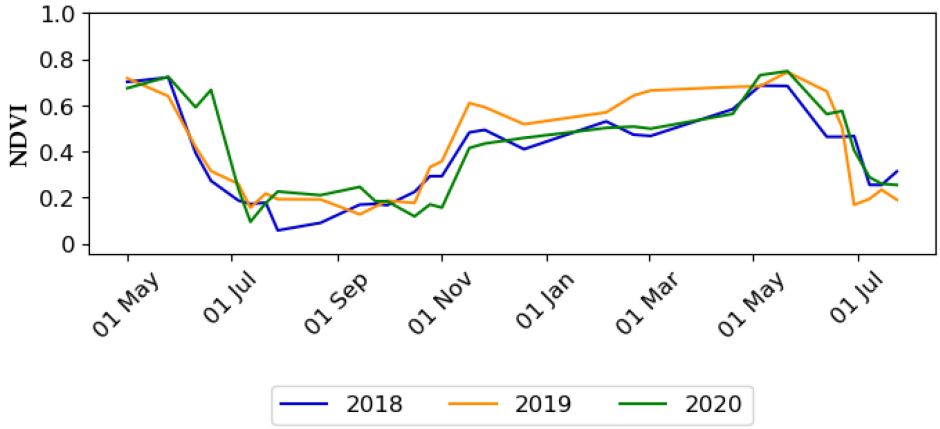

Fig. 5. NDVI temporal behavior over rapeseed fields in 2018, 2019, and 2020. The NDVI-values were calculated from Sentinel-2 images (S2), downloaded from the Theia website (https://www.theia-land.fr/).

with the LSTM-FCN (2%), showing higher variation in the accuracy across years. Concerning the precision and recall, the highest precision is achieved by RF (97.4%), but it also showed the lowest recall (92.7%). Meanwhile, the smallest difference between recall and precision is achieved by InceptionTime and MLP.

2) Rapeseed Fields Mapping Using Smaller Training Sample Size: The effect of four training sample sizes including 100, 300, 500, and 1000 on the accuracy of the rapeseed map is shown in Table V. In this case, the classification was performed using small training samples in order to mime the ratio between the rapeseed and nonrapeseed classes as found in the large annual

TABLE IV
ACCURACY ASSESSMENT OF RAPESEED CLASSIFICATION USING OUR FOUR ALGORITHMS

Metric	Algorithm	Mean	Min	Max
F1% - Rapeseed	**RF**	**95.0**	**94.2**	**95.5**
	MLP	**95.5**	**95.1**	**95.8**
	LSTM-FCN	**95.3**	**94.0**	**96.0**
	Inc-Time	**95.7**	**95.5**	**95.8**
Precision % - Rapeseed	RF	97.4	97.3	97.5
	MLP	95.5	95.2	95.7
	LSTM-FCN	95.9	95.4	96.6
	Inc-Time	95.3	94.7	95.7
Recall % - Rapeseed	RF	92.7	91.2	93.6
	MLP	95.5	95.1	95.8
	LSTM-FCN	94.6	92.7	96.3
	Inc-Time	96.1	95.8	96.5

Note: Mean = average value of each metric over all three years, Max = maximum value of each metric within three years, Min = minimum value of each metric.
The bold values indicate the highest performances.

TABLE V
EFFECT OF SAMPLE SIZE ON THE RAPESEED CLASSIFICATION ACCURACY

Metric	Algorithm	Mean-100 sample	Mean-300 sample	Mean-500 sample	Mean-1000 sample
F1 % - Rapeseed	**RF**	67.2	**90.1**	**91.1**	**92.9**
	MLP	14.7	54.0	65.6	85.2
	LSTM-FCN	39.1	29.0	29.7	69.6
	Inc-Time	59.3	**92.1**	**93.1**	**93.5**
Precision % - Rapeseed	RF	97.8	96.5	97.1	97.2
	MLP	9.4	71.3	95.2	95.7
	LSTM-FCN	43.4	59.6	59.1	93.2
	Inc-Time	62.1	94.8	95.2	94.7
Recall %- Rapeseed	RF	56.8	84.6	86.0	88.9
	MLP	52.4	45.1	51.9	77.2
	LSTM-FCN	44.7	21.7	23.2	58.3
	Inc-Time	59.7	89.7	91.3	92.5

The bold values indicate the highest performances.

sample dataset (imbalanced training data). For example, in the large dataset of the year 2018, the percentage of rapeseed and non-rapeseed classes was 3% and 97%, respectively, so in the case of classification of this year with the training sample size equal to 1000, the number of rapeseeds on training samples was 30 and nonrapeseed was 970. In Table V, the average accuracy metrics of the three years 2018, 2019, and 2020 are presented (e.g., Mean-100 samples is the average of each metric over three years of classification using 100 ground samples). Table V shows that the Inception Time and RF provide higher accuracy metrics than the other algorithms. Both RF and Inception Time yielded F1 values greater than 90% when using a sample size greater than 300. In the case of 100 samples, these two algorithms respectively showed F1 values of 67.2% and 59.3%. For RF, the reason behind the lower F1 value with a sample size of 100 is the lower recall value, and both lower precision and recall for the Inception Time. Therefore, both Inception Time and RF can produce accurate rapeseed maps using training sample size of 300 samples or bigger, while in the case of 100 samples the accuracy of their results are not high (but still better than the two other algorithms). Among the ANNs algorithms, LSTM-FCN presents the lowest accuracy between the two other algorithms (F1 value below 40% with a sample size smaller than 1000, and F1 value below 69% with 1000 samples). In addition, both the recall and precision of this algorithm are lower than 60% and 40% respectively when the sample size is less than 1000. Using the MLP, when the sample size increases from 100 to 1000, the mean F1 value increases from 14.7% to 85.2% (F1 value of 54.0% and 65.6% with a sample size of 300 and 500, respectively).

TABLE VI
ASSESSMENT OF RAPESEED CLASSIFICATION ACCURACY USING DIFFERENT YEARS FOR TRAINING AND FOR TESTING

Metric	Algorithm	Mean	Min	Max
F1% - Rapeseed	RF	87.1	79.1	92.8
	MLP	85.5	82.6	89.0
	LSTM-FCN	89.3	84.1	93.4
	Inc-Time	**92.7**	**90.7**	**94.9**
Precision % - Rapeseed	RF	98.2	97.3	99.2
	MLP	91.7	82.6	97.4
	LSTM-FCN	96.8	94.0	98.4
	Inc-Time	97.2	95.6	97.8
Recall % - Rapeseed	RF	78.9	65.9	88.0
	MLP	80.9	75.2	89.8
	LSTM-FCN	83.6	74.5	93.2
	Inc-Time	88.7	85.1	94.3

Note: Mean = average of each metric from all six combinations of training and testing years, Max = maximum value of each metric from the six combinations, Min = minimum value of each metric from the six combinations.
The bold values indicate the highest performances.

3) Transferability of the Models Using Different Years for Training and Testing: The accuracy of rapeseed fields mapping using different years for training and testing was evaluated. This investigation is of some interest in the absence of ground sampling over the same territory for certain years. Thus, the possibility of creating the rapeseed map using the ground samples of the other years was tested. The transferability of the models was carried out using large sample sizes since results of Section IV-B2 of results showed that LSTM-FCN and MLP did not give accurate results with smaller sample sizes. To evaluate the ability of the AI algorithms to map the rapeseed fields for each year using the ground sample of other years, six combinations of train and test data were created (train on one year and apply on the remaining two years). The mean, maximum, and minimum accuracy metrics of these combinations are presented in Table VI. As shown in this table, RF, MLP, LSTM-FCN, and InceptionTime yielded F1 value greater than 85% (min-values) using different years of training and testing. These high values of F1 for the four tested models show that it is possible to transfer a model from one year to another for mapping rapeseed fields using S1 time series data. The comparison between the four algorithms shows

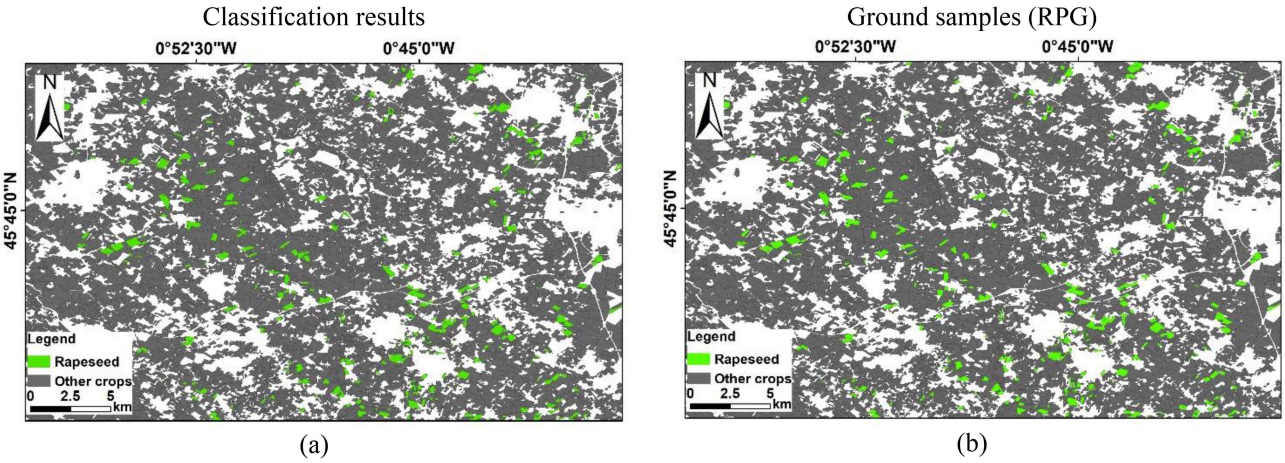

Fig. 6. Comparison between rapeseed maps created by InceptionTime and ground samples (RPG) for a part of the study site, using different years for training and testing. (a) Training 2018/test 2019. (b) Ground samples of 2019. Rapeseed fields are colored green, other crops are colored grey.

that the InceptionTime provided mean F1 value higher than other algorithms. The smallest differences between the minimum and maximum of F1 were also achieved with the InceptionTime algorithm (4% difference between F1 min and max). This means that high accuracy was achieved with InceptionTime in all six combinations of training and test years. LSTM-FCN provided a mean F1 value of 89.3% which indicates that this algorithm was also capable of providing accurate rapeseed fields map for each year by training it using ground samples of the other years. MLP showed the lowest F1 values (mean F1 equal to 85.5). On the other hand, RF obtained a mean F1 value of 87.1% but it showed the highest difference between the minimum and maximum of F1 value (13.7%). This difference for both MLP and RF algorithms was due to the low minimum recall (80.9% and 78.9% with MLP and RF respectively). Therefore, RF and MLP were less accurate in terms of transferability of the model from one year to another.

To better appreciate the spatial accuracy of the transferability of the models, the rapeseed maps were created by Inception time (as the algorithm with the best accuracy outcome) was compared to the ground samples (RPG). Fig. 6 shows the rapeseed field map for 2019 using the ground samples of 2018. Fig. 7(a) and (b) illustrate respectively the rapeseed field maps for 2020 using the ground samples of 2018 and 2019. Also, the corresponding ground reference maps for 2019 and 2020 are presented respectively by Figs. 6(b) and 7(c). The rapeseed fields were mostly classified correctly compared to the reference data. The analysis of these maps shows that the rapeseed fields incorrectly classified as nonrapeseed have a small area. For the rapeseed map of 2019 using the ground samples of 2018, 6.5% of the rapeseed fields were misclassified as nonrapeseed, of which 51% had an area smaller than 0.5 ha and 18% an area between 0.5 and 1 ha. To map the rapeseed fields of 2020 from the ground samples of 2018, 5.1% of the rapeseed fields were incorrectly classified as nonrapeseed, of which 47% had an area smaller than 0.5 ha, and 26% an area between 0.5 and 1 ha. Finally, 6.7% of the rapeseed fields were misclassified in 2020 when the ground samples of 2019 were used, of which 37% had an area smaller than 0.5 ha and 32% an area between 0.5 and 1 ha. In conclusion, the misclassifications were therefore mainly occurred in the detection of rapeseed fields smaller than 1 ha (about 70% of the misclassification), which could be a consequence of the higher edge effect in small fields, as well as the lower number of S1 pixels used to calculate the mean of the backscatter signals due to the high speckle effect

4) Effect of Number of Images in Time Series and the Shift in the Phenological Cycle Between Training and Test Years on Transferability of the Models: Two important arguments about the transferability of the models were addressed, including the effect of the number of images in the S1 time series and the effect of the shift in the phenological stage of rapeseed between training and test years.

a) Using a reduced number of S1 images (only one orbit): The effect of the number of S1 images on the transferability of models for mapping the rapeseed fields was assessed by considering only one orbit (orbit 8) out of the 3 orbits of our initial time series. This use case allows us to see whether, in the event of a reduction in the revisit time of S1 (failure of one of the two satellites, which is currently the case), the accuracy of the rapeseed fields classification remains good for the different algorithms.

Table VII shows the performance of each algorithm using one and three orbits where the year 2018 is set as a training year and the years 2019 and 2020 were considered as the testing years The results in this table correspond to the average performance obtained over 2019 and 2020. As Table VII shows, the performance of InceptionTime and LSTM-FCN decreased when only one orbit was used compared to the accuracy obtained using three orbits. In fact, the F1 value using InceptionTime decreased from 94.1% with three orbits to 77.1% with only one orbit (17.6% reduction). Similarly, LSTM-FCN showed a reduction in F1 from 88.3% using three orbits to 72.1% using one orbit (16.2% reduction). Looking at the recall and precision, it can be seen that for InceptionTime the reduction occurred in both recall and precision, while for LSTM-FCN the reduction in recall caused the reduction in F1 compared to the use of three

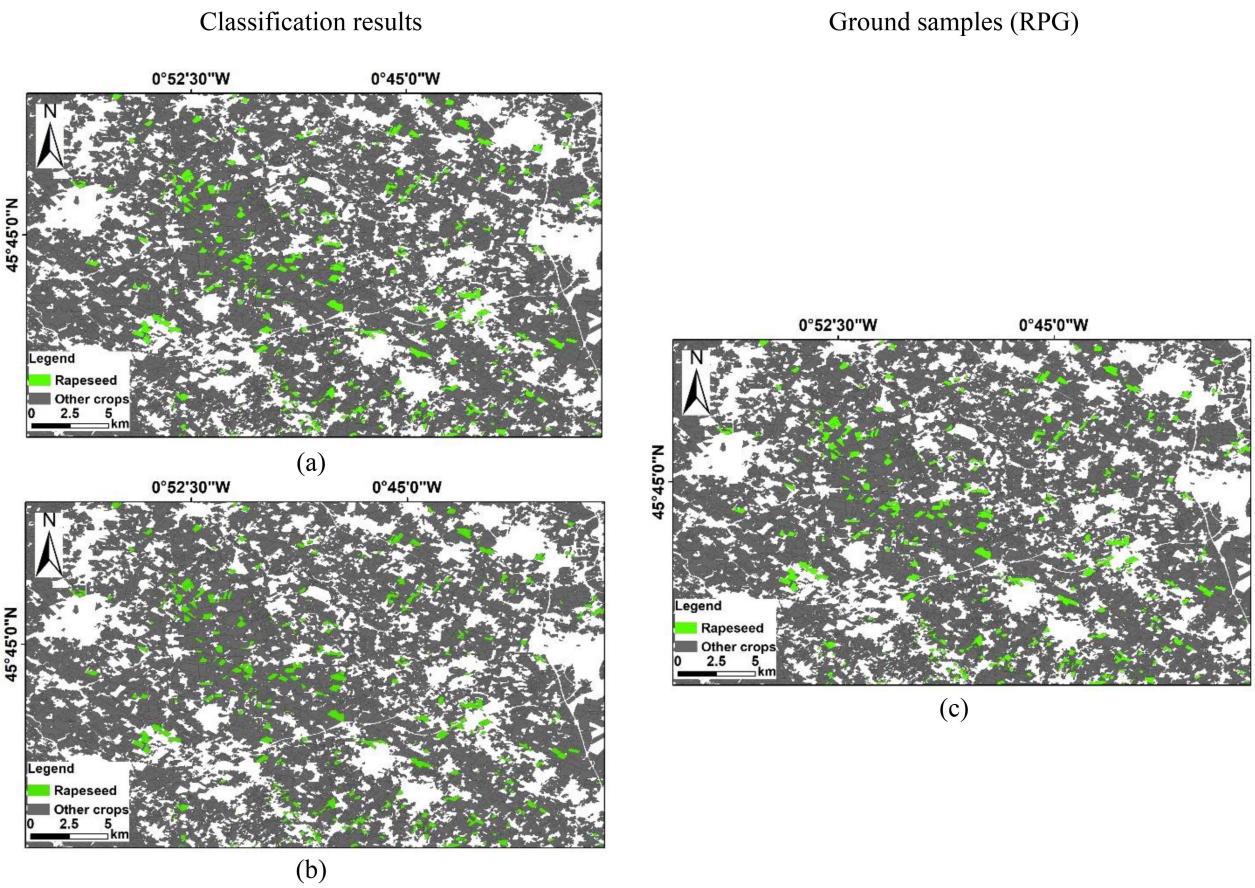

Fig. 7. Comparison between rapeseed maps created by InceptionTime and ground samples (RPG) for a part of the study site, using different years for training and testing. (a) Training 2018/test 2020. (b) Training 2019/test 2020. (c) Ground samples of 2020. Rapeseed fields are colored green, other crops are colored grey.

orbits. The reduction in the number of S1 images in the time series had less impact on the MLP and RF algorithms than that on the LSTM-FCN and InceptionTime where the reduction in F1 was of an order of 5% and 0.5% using one orbit instead of three orbits for MLP and RF, respectively. However, RF with an F1 value of 89.1% had better performance when compared to MLP with an F1 value of 80.0%. The lower precision (72.3%) compared to the recall (92.4%) caused the lower F1 value using MLP when compared to RF. In conclusion, using one orbit of S1 time series, not only the performance of RF remains more than acceptable, it also outperforms the other three ANNs algorithms (MLP, LSTM-FCN, InceptionTime).

b) Using a shift in the phenological cycle between training and test years: Table VIII shows the results of the accuracy assessment of the transferability of the models with the simulation of the 15-day and 30-day shifts in the phenological cycle of rapeseed in 2018 as training data without any modification in the 2020 dataset as test. InceptionTime and LSTM-FCN provided the best accuracy among other algorithms with nearly similar accuracy metrics with and without the time shift. With a 15-days shift in the phenological cycle of rapeseed, the InceptionTime algorithm gave rapeseed fields map with F1 value equal to 92.6% (the F1 value of 94.3% for the same combination of years without shift). In the case of classification using InceptionTime with a 30-days shift, F1 reached 89.3%. LSTM-FCN gave F1 values of 85.6% and 84.7% for 15- and 30-days shift, respectively (the F1 value of 87.2% for the same combination of years without shift). On the other hand, lower performance was obtained for RF and MLP achieving F1 values of 34.6% and 29.1%, respectively, for 15 days' shift. For a 30 days' shift, RF and MLP had F1 values lower than 5%. In the case of 15 days shift the low value of recall (below 20%) caused the poor performance of both RF and MLP, whereas in the case of 30 days' shift, both recall (close to 0%) and precision (55.8% and 18.9% for RF and MLP, respectively) were low for these two algorithms. Thus, in the case of a phenological shift between the training year and the test year, RF and MLP were not able to produce accurate rapeseed fields map. However, LSTM-FCN and InceptionTime were capable of maintaining good accuracy in the presence of a phenological shift between the training and mapping years.

V. Discussion

A. S1 Temporal Behavior

The S1 backscatter analysis [see Fig. 4(a) and (b)] showed that the radar signal at plot scale is affected by rainfall events, especially in the early growth stage when the vegetation cover is not very dense and the effect of the soil surface condition is greater than the effect of the vegetation cover.

TABLE VII
EFFECT OF S1 ACQUISITION DENSITY ON THE ACCURACY OF RAPESEED FIELDS MAPPING

Metric	Algorithm	One orbit (2018/2019, 2018/2020)	Three orbits (2018/2019, 2018/2020)
F1 % - Rapeseed	**RF**	**89.1**	94.1
	MLP	80.0	80.5
	LSTM-FCN	72.1	88.3
	Inc-Time	77.1	94.7
Precision % - Rapeseed	RF	93.9	97.4
	MLP	72.3	83.4
	LSTM-FCN	92.5	89.0
	Inc-Time	77.9	95.2
Recall %- Rapeseed	RF	84.9	90.8
	MLP	92.4	78.4
	LSTM-FCN	63.9	88.5
	Inc-Time	82.8	92.9

Note: Training was performed using the 2018 dataset and testing was performed on the 2019 and 2020 datasets. The two cases used are data corresponding to orbit 8 (one orbit) and data corresponding to orbits 8, 30 and 81 (three orbits). The results correspond to the average performance obtained over 2019 and 2020.
The bold values indicate the highest performances.

TABLE VIII
RESULTS OBTAINED BY APPLYING A TIME SHIFT OF 15 AND 30 DAYS ON THE TRAINING DATASET OF 2018, WITHOUT MODIFYING THE TEST DATASET OF 2020

Metric	Algorithm	Without shift	15 days shift	30days shift
F1% - Rapeseed	RF	95.0	34.6	0.2
	MLP	83.3	29.1	5.3
	LSTM-FCN	87.2	85.6	84.7
	Inc-Time	94.3	**92.6**	**89.3**
Precision % - Rapeseed	RF	97.4	97.9	55.8
	MLP	81.5	61.2	18.9
	LSTM-FCN	84.4	84.0	83.0
	Inc-Time	94.3	93.8	89.2
Recall % - Rapeseed	RF	92.7	21.3	0.1
	MLP	85.3	19.3	3.1
	LSTM-FCN	94.3	91.9	85.8
	Inc-Time	94.3	91.7	89.6

Note: Without shift = The current phenological cycle of rapeseed in the datasets used for training and testing.
The bold values indicate the highest performances.

The temporal behavior of VHp and VVp over rapeseed fields showed four phases which are related to the four main phenological stages of rapeseed [4], [12], [50]. However, the fluctuation of the VHp channel is stronger with the growth cycle of rapeseed. This was expected, as the VH is well known to be more sensitive to the vegetation cover and its geometrical structure than the VV polarization which is more sensitive to the soil moisture [51]. During the leaf production between September and November, both polarizations increase according to biomass growth [14], [20]. When the rapeseed growth rate is low due to the cold weather between November and March the value of VHp and VVp is stable. During the rapid spring growth of rapeseed between March and June, there is a strong increase in VHp and VVp, corresponding to the stem elongation, inflorescence emergence, and fruit development [4], [12]. According to Mercier et al. [20] and Veloso et al. [12], the peak in signal is due to the higher biomass, as well as taller rapeseed and randomly oriented branches, resulting in higher backscatter due to the double bounce effect. With the onset of senescence in June and July, both VHp and VVp decrease strongly due to the lower water volume in the top layer of rapeseed and higher soil contribution than the vegetation contribution in the S1 backscattering signal (higher S1 signal penetration) [20]. The unique behavior of the S1 time series according to the phenological cycle of rapeseed, especially the high peak in May and early June is valuable for rapeseed fields mapping as shown in this study and previous studies [8], [12]. Therefore, methods such as the DL algorithms, which are based on the end-to-end learning from the input data, can take advantage of this behavior of S1 signals to distinguish the rapeseed fields.

B. Rapeseed Mapping

Although the mapping of rapeseed fields was carried out in previous studies, this article has addressed several functional arguments to facilitate the detection of rapeseed fields. First, by presenting the algorithms capable of producing the rapeseed maps using a S1 time series with a high accuracy and second by developing different solutions for producing the rapeseed fields map when there are not enough ground samples. In this aim, four algorithms were used to classify the S1 time series, including a machine learning algorithm, called RF, and three DL algorithms, namely MLP, LSTM-FCN, and InceptionTime. RF is a well-known method in remote sensing applications due to its high performance [28], [37], [38]. Therefore, as in previous studies such as the one by Zhong et al. [25], RF provides the baseline for all other classifications in the current paper. In addition, MLP, which is a public simple deep ANNs, and LSTM-FCN and InceptionTime, which are specialized for time series analysis, were also used for the classification of rapeseed fields. Our results showed how AI algorithms offer specific advantages for remote sensing applications. These advantages are discussed in this section.

1) Application of AI in Rapeseed Fields Mapping: All four algorithms including RF, MLP, LSTM-FCN, and InceptionTime gave high accuracy metrics when detecting rapeseed fields utilizing an S1-derived time series, using samples from the same year for training and for testing (mean F1 value close to 95%). Among the four algorithms that were applied in this article, InceptionTime showed the best performance in classifying the rapeseed fields using training and testing data from the same year compared to the RF, MLP, LSTM-FCN. Not only did InceptionTime provide the highest F1 value (95.7%), it also provided the most stable performance across the different tested years. Fawaz

et al. [40] mentioned that InceptionTime has less variation in results, thanks to the application of multiple inception networks in its architecture.

By using only S1 time series better results were obtained in this article compared to Mercier et al. [20] who reported lower accuracy (kappa value of 0.63) by classifying rapeseed fields using only S1 time series and an incremental method developed by Mercier et al. [52]. In fact, previous papers have either used optical images alone or some combination of radar and optical images to achieve high accuracy for rapeseed detection [19], [53]. This article provides a high accuracy using only S1 time series, which reduces the image processing and data analysis time. Waldhoff et al. [54] integrated ASTER, Landsat-5-8, IRS-P6, SPOT-6/7, and RapidEye images for mapping the rapeseed fields in western Germany and obtained an F1 value of 86.2% using the multidata approach proposed by Bareth [55]. Han et al. [22] achieved F1 values between 0.84 and 0.91 using a combination of S1 and S2 data from 33 countries using the pixel- and phenology-based method. One of the strength points of the current study is thus the ability to obtain the optimal rapeseed mapping accuracy relying only on one satellite data source (the S1 time series) which is in free and in open access mode.

2) Solutions to Ground Sampling Constraints: The difficulties of ground sampling due to time and budget constraints, poor accessibility to the study area as well as the absence of historical training samples for each year have been mentioned in similar remote sensing applications for land cover mapping [56], [57], [58]. Based on the results of the current paper two solutions could be proposed to mitigate the above-mentioned constraints.

Our first solution to the ground sampling constraints is to develop a model over one year and apply it to other years without having to train it again. The results of the current study showed that using all the four algorithms, it is possible to accurately detect the rapeseed fields, using different years for training and for testing. InceptionTime showed the best performance when compared to the other algorithms by providing the highest F1 (92.7%), as well as the smallest difference between minimum and maximum of accuracy metrics (over our six combinations of training and test years). This means that the InceptionTime algorithm can use what it learns in each year to accurately classify the next or previous year. The F1-score obtained in the current study with InceptionTime (92.7%) is higher than methods used in previous studies to classify the time series using historical data for training. In Lin et al. [56], F1 value was 88% and 85% for mapping, respectively, corn and soybeans using Sentinel-2 and Landsat optical time series. In addition, classification using InceptionTime which learns the backscatter of rapeseed directly from the satellite images is not as complicated as the decision boundary-based approaches which select thresholds for each crop from the historical samples and apply them to the target year [38], [58], [59], [60]. Meanwhile, LSTM-FCN also showed the capability of producing accurate rapeseed fields map for each year using the ground samples of other years for training with a mean F1 value of 89.3%. Looking at the results of RF, despite the high mean value of F1 equal to 87.1%, this algorithm performs less well when compared to the previously mentioned ANNs algorithms in the case of temporal transfer due to 13.7% difference between the minimum and maximum of F1 values. Meanwhile, MLP had the worst performance with the lowest F1 value among other algorithms in the transfer classification (mean F1 of 85.5%).

In order to be sure about the possibility of obtaining high accuracy results with our first solution to ground sampling constraints (creating the rapeseed map using the ground samples of the other years), it is worth addressing two important arguments, including the effect of the shift in the phenological cycle of rapeseed between training and test years, and the effect of the number of images in the S1 time series. The results obtained with 15-days and 30-days shift in the rapeseed growth cycle between training and test datasets showed that using InceptionTime and LSTM-FCN, it remains possible to classify the rapeseed fields with an F1 value higher than 84.7% when there is a shift of up to 30 days between the training and test years (F1 value higher than 85.6% for a shift of 15 days). However, the F1 value of InceptionTime was 5% higher than LSTM-FCN. On the other hand, RF and MLP had poor accuracy (F1 value less than 35% and 5%, respectively, for a shift of 15 and 30 days) and thus they cannot be used in the case of temporal transfer when there is shift in growth cycle of rapeseed between the training and test year. These findings provide functional advantages that facilitate the procurement of information about rapeseed which is a strategic crop in the global trade and plays an important role in global food security. Indeed, thanks to the temporal transferability of InceptionTime and LSTM-FCN, even with a 30 days shift in the growth cycle between training and test data, it is still possible to get accurate information on rapeseed cultivation areas in the main rapeseed producing countries regardless of challenging conditions (for example the war in Ukraine) which cause inaccessibility to large cultivation areas. In addition, these results show that it is possible to map the rapeseed from ground samples of previous years (same region) or collected on other regions in the same agro-climatic zone, where the shift in the growth stage of rapeseed is lower than 30 days. From a functional point of view, the rapid retrieval of information on the area of cultivation is always important for the decision makers [20], [61]. So, the classification of time series using the ground samples collected in the previous years with a shift of less than 30 days would be worthwhile. Furthermore, as the phenological period is delayed in cold regions compared to warmer regions, the possibility of temporal transfer algorithms is a crucial argument for the accurate classification of rapeseed over large regions or in the case of climate change [4].

On the other hand, when the number of images in time series was reduced, the performance of the classification with InceptionTime and LSTM-FCN decreased for transferability of model of around 16% (77.1% and 72.1%, respectively), whereas the performance of RF and MLP did not decrease significantly. However, RF gave an F1 value of 89.1% which was higher than all the ANNs algorithms. Therefore, a reduction in the revisit time of S1 reduces the accuracy of InceptionTime and LSTM-FCN. Thus, in the case of large reduction in the number of images in the time series, RF will be the best choice to use when training and testing using different years without phenological shift.

TABLE IX
RECOMMENDATION ON THE USE OF OUR FOUR ALGORITHMS ACCORDING TO THE CONSTRAINTS IN THE FIELD SAMPLES

	Temporal transfer				Small sample size			
	Without shift	15 days shift	30 days shift	Reduction of the number of S1 images	100 samples	300 samples	500 samples	1000 samples
RF	✓	⦸	⦸	✓	✓	✓	✓	✓
MLP	✓	⦸	⦸	○	⦸	⦸	⦸	✓
LSTM-FCN	✓	✓	✓	○	⦸	⦸	⦸	⦸
InceptionTime	✓	✓	✓	○	○	✓	✓	✓

Our second solution to the ground sample constraints is to propose a method that gives accurate results even when using a small training sample size. Therefore, the effect of training sample size on the performance of the AI classifiers was evaluated using four sizes of ground samples, including 100, 300, 500, and 1000. The results obtained in the case of small sample size showed that RF and InceptionTime classify the rapeseed with high accuracy metrics when the training sample size is greater than 300 (F1-score higher than 90). However, when using only 100 samples, InceptionTime did not perform better than F1 value of 59.3. The accurate classification performed by InceptionTime using sample sizes greater than 300 showed the lower effect of sample size on the performance of which confirms the stability of the results of this algorithm compared to the other two ANNs. Although DL is known as a method that requires a large training dataset, Fawas et al. [40] mentioned that providing the accurate results using the small sample size by InceptionTime as another advantage of assembling the several inception networks in this algorithm. In the case of a sample size of 100, RF gave an F1 value 7% higher than InceptionTime. RF as a machine learning model, provides F1 values between 90% and 92% using the sample sizes larger than 300 samples (300, 500, and 1000), which shows that when the number of samples increases, no great improvement occurs in the accuracy of classification by RF. On the contrary, the performance of LSTM-FCN and MLP decreased dramatically using the sample size smaller than 1000, therefore, these two algorithms are not recommended for rapeseed classification in the case of small sized samples.

In summary, taking into account the effect of the phenological cycle shift, the number of S1 images, and the size of training samples on the ability of our four algorithms to provide a solution to the constraints concerning the ground samples, Table IX illustrates the recommended algorithms for each use case. It is possible to use all algorithms in the case of the temporal transfer when there is no shift in the training and test data. InceptionTime can be used in all tested cases, although its performance is not the highest for the case of 100 samples, and temporal transfer with a smaller number of S1 images. RF could be used for all tested cases except when there is phenological shift. LSTM-FCN is useful for temporal transfer even when there is a shift in the phenological cycle. But, MLP can only be used in the case of 1000 samples or temporal transfer without phenological shift. This means that MLP cannot be widely used as a functional algorithm in the case of sample size constraints. This can be due to its simple ANNs architecture.

VI. CONCLUSION

This article presents an assessment of artificial intelligence algorithms for mapping rapeseed fields using S1 time series data. The accuracy of rapeseed mapping was assessed for four algorithms considering

1) the effect of the sample size for training;
2) the ability to deploy a model trained on one year on other years;
3) the effect of the number of available S1 images in the time series;
4) the effect of a possible phenological shift between studied years.

In the case where large databases (nearly 100 000 samples) are used for training, this article demonstrated that RF, InceptionTime, LSTM-FCN, and MLP were capable of accurately mapping the rapeseed fields using only S1 SAR time series using the same year for training and for testing (F1 score between 95.0% for RF and 95.7% for InceptionTime). However, using a smaller sample size (but no less than 300 samples), RF and InceptionTime gave better results (F1 score higher than 92.0% for InceptionTime and 90.0% for RF) compared to the LSTM-FCN and MLP (F1 score higher than 29.0% for LSTM-FCN and 53.9% for MLP). It was also shown that all four algorithms were able to produce an accurate map of rapeseed fields in the case of temporal transfer when the training and test data were selected from different years (F1 score between 85.5% for MLP and 92.7% for InceptionTime). The number of S1 images in the time series is an important dimension for temporal transferability, especially for the two ANNs algorithms that are specialized in time series analysis (InceptionTime, LSTM-FCN), because the accuracy of classification using these two algorithms dropped down when the number of images in the time series decreased (a decrease of 16.9% for InceptionTime, 15.9% for LSTM-FCN). However, RF performed well even when the number of images in the time series decreased (F1 score of 87.1% with three orbits, and 85.1% with one orbit). In the case of a phenological shift between years, only InceptionTime and LSTM_FCN (F1 score about 89.3% with InceptionTime and 84.6% with LSTM-FCN for phenological shift of 30 days) achieved good accuracy in rapeseed field mapping, whereas RF and MLP were not suitable for the case of a phenological shift between the training year and the mapping year. It is worth noting that in this article, the default parameter values for the algorithms were used with the aim to have a unique baseline for the comparability of the performance of the algorithms in each scenario. However, tuning of the

algorithms can be applied in further studies. Indeed, adjusting these parameters based on the data could improve the model's performance and ensure optimal results. In addition, to tackle more challenging transfer scenarios between training and test datasets, an interesting avenue for future work would be to apply more robust training techniques (e.g., with data augmentation) and account for domain changes beyond time lags. The findings of this article are not only useful for remote sensing researchers, but they also facilitate the detection of rapeseed fields for other stakeholders such as policy makers and insurance companies, even with the constraints of collecting ground samples for each year.

ACKNOWLEDGMENT

The authors would like to also thank the European Space Agency for providing the S1 images.

REFERENCES

[1] Y. Ma et al., "Spatiotemporal analysis and war impact assessment of agricultural land in Ukraine using RS and GIS technology," *Land (Basel)*, vol. 11, no. 10, Oct. 2022, Art. no. 1810, doi: 10.3390/land11101810.

[2] S. Chen et al., "Two-stepwise hierarchical adaptive threshold method for automatic rapeseed mapping over Jiangsu using harmonized landsat/sentinel-2," *Remote Sens. (Basel)*, vol. 14, no. 11, Jun. 2022, Art. no. 2715, doi: 10.3390/rs14112715.

[3] United States Department of Agriculture, "USDA Crop Explorer - Commodity View," *USDA Crop Explorer*. Accessed: Feb. 2023. [Online]. Available: https://ipad.fas.usda.gov/cropexplorer/cropview/commodityView.aspx?cropid=2226000

[4] H. Zhang, W. Liu, and L. Zhang, "Seamless and automated rapeseed mapping for large cloudy regions using time-series optical satellite imagery," *ISPRS J. Photogrammetry Remote Sens.*, vol. 184, pp. 45–62, Feb. 2022, doi: 10.1016/j.isprsjprs.2021.12.001.

[5] W. Liu and H. Zhang, "Mapping annual 10 m rapeseed extent using multi-source data in the Yangtze River Economic Belt of China (2017–2021) on Google Earth Engine," *Int. J. Appl. Earth Observation Geoinf.*, vol. 117, Mar. 2023, Art. no. 103198, doi: 10.1016/j.jag.2023.103198.

[6] Z. Pan, J. Huang, and F. Wang, "Multi range spectral feature fitting for hyperspectral imagery in extracting oilseed rape planting area," *Int. J. Appl. Earth Observation Geoinf.*, vol. 25, pp. 21–29, Dec. 2013, doi: 10.1016/j.jag.2013.03.002.

[7] J. Chen and A. Zipf, "DeepVGI: Deep learning with volunteered geographic information," in *Proc. 26th Int. World Wide Web Conf. Companion, Int. World Wide Web Conf. Steering Committee*, 2017, pp. 771–772, doi: 10.1145/3041021.3054250.

[8] R. d'Andrimont, M. Taymans, G. Lemoine, A. Ceglar, M. Yordanov, and M. van der Velde, "Detecting flowering phenology in oil seed rape parcels with Sentinel-1 and -2 time series," *Remote Sens. Environ.*, vol. 239, Mar. 2020, Art. no. 111660, doi: 10.1016/j.rse.2020.111660.

[9] L. Wang, J. Wang, Z. Liu, J. Zhu, and F. Qin, "Evaluation of a deep-learning model for multispectral remote sensing of land use and crop classification," *Crop J.*, vol. 10, no. 5, pp. 1435–1451, Oct. 2022, doi: 10.1016/j.cj.2022.01.009.

[10] J. Han, Z. Zhang, and J. Cao, "Developing a new method to identify flowering dynamics of rapeseed using landsat 8 and sentinel-1/2," *Remote Sens. (Basel)*, vol. 13, no. 1, pp. 1–18, Jan. 2021, doi: 10.3390/rs13010105.

[11] D. Wang et al., "A regional mapping method for oilseed rape based on HSV transformation and spectral features," *ISPRS Int. J. Geo-Inf.*, vol. 7, no. 6, Jun. 2018, Art. no. 224, doi: 10.3390/ijgi7060224.

[12] A. Veloso et al., "Understanding the temporal behavior of crops using Sentinel-1 and Sentinel-2-like data for agricultural applications," *Remote Sens. Environ.*, vol. 199, pp. 415–426, Sep. 2017, doi: 10.1016/j.rse.2017.07.015.

[13] J. Cable, J. Kovacs, X. Jiao, and J. Shang, "Agricultural monitoring in northeastern Ontario, Canada, using multi-temporal polarimetric RADARSAT-2 data," *Remote Sens. (Basel)*, vol. 6, no. 3, pp. 2343–2371, Mar. 2014, doi: 10.3390/rs6032343.

[14] R. Fieuzal, F. Baup, and C. Marais-Sicre, "Monitoring wheat and rapeseed by using synchronous optical and radar satellite data—From temporal signatures to crop parameters estimation," *Adv. Remote Sens.*, vol. 2, no. 2, pp. 162–180, 2013, doi: 10.4236/ars.2013.22020.

[15] H. McNairn, X. Jiao, A. Pacheco, A. Sinha, W. Tan, and Y. Li, "Estimating canola phenology using synthetic aperture radar," *Remote Sens. Environ.*, vol. 219, pp. 196–205, Dec. 2018, doi: 10.1016/j.rse.2018.10.012.

[16] G. Wiseman, H. McNairn, S. Homayouni, and J. Shang, "RADARSAT-2 polarimetric SAR response to crop biomass for agricultural production monitoring," *IEEE J. Sel. Topics Appl. Earth Observ. Remote Sens.*, vol. 7, no. 11, pp. 4461–4471, Nov. 2014.

[17] S. Yang, L. Gu, X. Li, T. Jiang, and R. Ren, "Crop classification method based on optimal feature selection and hybrid CNN-RF networks for multi-temporal remote sensing imagery," *Remote Sens. (Basel)*, vol. 12, no. 19, Sep. 2020, Art. no. 3119, doi: 10.3390/rs12193119.

[18] J. M. Lopez-Sanchez, F. Vicente-Guijalba, J. D. Ballester-Berman, and S. R. Cloude, "Polarimetric response of rice fields at C-band: Analysis and phenology retrieval," *IEEE Trans. Geosci. Remote Sens.*, vol. 52, no. 5, pp. 2977–2993, May 2014, doi: 10.1109/TGRS.2013.2268319.

[19] F. Mouret, M. Albughdadi, S. Duthoit, D. Kouamé, G. Rieu, and J. Y. Tourneret, "Outlier detection at the parcel-level in wheat and rapeseed crops using multispectral and SAR time series," *Remote Sens. (Basel)*, vol. 13, no. 5, pp. 1–25, Mar. 2021, doi: 10.3390/rs13050956.

[20] A. Mercier et al., "Evaluation of Sentinel-1 & 2 time series for predicting wheat and rapeseed phenological stages," *ISPRS J. Photogrammetry Remote Sens.*, vol. 163, pp. 231–256, May 2020, doi: 10.1016/j.isprsjprs.2020.03.009.

[21] A. Allies et al., "Evaluation of multiorbital SAR and multisensor optical data for empirical estimation of rapeseed biophysical parameters," *IEEE J. Sel. Topics Appl. Earth Observ. Remote Sens.*, vol. 14, pp. 7268–7283, 2021.

[22] J. Han et al., "The RapeseedMap10 database: Annual maps of rapeseed at a spatial resolution of 10 m based on multi-source data," *Earth Syst. Sci. Data*, vol. 13, no. 6, pp. 2857–2874, Jun. 2021, doi: 10.5194/essd-13-2857-2021.

[23] M. Campos-Taberner et al., "Understanding deep learning in land use classification based on Sentinel-2 time series," *Sci. Rep.*, vol. 10, no. 1, Dec. 2020, Art. no. 17188, doi: 10.1038/s41598-020-74215-5.

[24] A. Vali, S. Comai, and M. Matteucci, "Deep learning for land use and land cover classification based on hyperspectral and multispectral earth observation data: A review," *Remote Sens.*, vol. 12, no. 15, Aug. 2020, Art. no. 2495, doi: 10.3390/RS12152495.

[25] L. Zhong, L. Hu, and H. Zhou, "Deep learning based multi-temporal crop classification," *Remote Sens. Environ.*, vol. 221, pp. 430–443, Feb. 2019, doi: 10.1016/j.rse.2018.11.032.

[26] P. Hao, M. Wu, Z. Niu, L. Wang, and Y. Zhan, "Estimation of different data compositions for early-season crop type classification," *PeerJ*, vol. 6, May 2018, Art. no. e4834, doi: 10.7717/peerj.4834.

[27] P. Griffiths, C. Nendel, and P. Hostert, "Intra-annual reflectance composites from Sentinel-2 and Landsat for national-scale crop and land cover mapping," *Remote Sens. Environ.*, vol. 220, pp. 135–151, Jan. 2019, doi: 10.1016/j.rse.2018.10.031.

[28] V. F. Rodriguez-Galiano, M. Chica-Olmo, F. Abarca-Hernandez, P. M. Atkinson, and C. Jeganathan, "Random forest classification of mediterranean land cover using multi-seasonal imagery and multi-seasonal texture," *Remote Sens. Environ.*, vol. 121, pp. 93–107, Jun. 2012, doi: 10.1016/j.rse.2011.12.003.

[29] S. Meng, Y. Zhong, C. Luo, X. Hu, X. Wang, and S. Huang, "Optimal temporal window selection for winter wheat and rapeseed mapping with Sentinel-2 images: A case study of Zhongxiang in China," *Remote Sens. (Basel)*, vol. 12, no. 2, Jan. 2020, Art. no. 226, doi: 10.3390/rs12020226.

[30] D. Ienco, R. Interdonato, R. Gaetano, and D. Ho Tong Minh, "Combining Sentinel-1 and Sentinel-2 satellite image time series for land cover mapping via a multi-source deep learning architecture," *ISPRS J. Photogrammetry Remote Sens.*, vol. 158, pp. 11–22, Dec. 2019, doi: 10.1016/j.isprsjprs.2019.09.016.

[31] S. Skakun et al., "Early season large-area winter crop mapping using MODIS NDVI data, growing degree days information and a Gaussian mixture model," *Remote Sens. Environ.*, vol. 195, pp. 244–258, Jun. 2017, doi: 10.1016/j.rse.2017.04.026.

[32] C. Zhang et al., "Joint deep learning for land cover and land use classification," *Remote Sens. Environ.*, vol. 221, pp. 173–187, Feb. 2019, doi: 10.1016/j.rse.2018.11.014.

[33] J. Jagannathan and C. Divya, "Deep learning for the prediction and classification of land use and land cover changes using deep convolutional neural network," *Ecol. Inform.*, vol. 65, Nov. 2021, Art. no. 101412, doi: 10.1016/j.ecoinf.2021.101412.
[34] D. Kumar Sahadevan, S. Rao Sitiraju, S. Dinesh Kumar, S. Srinivasa Rao, and J. R. Sharma, "Radar vegetation index as an alternative to NDVI for monitoring of soyabean and cotton new findings on course of river Sarasvati view project NWDPRA view project radar vegetation index as an alternative to NDVI for monitoring of soyabean and cotton," in *Proc. XXXIII INCA Int. Congr. (Indian Cartographer)*, Jodhpur, India, 2013, pp. 19–21. [Online]. Available: http://earthexplorer.usgs.gov/
[35] D. Wang, W. Cao, F. Zhang, Z. Li, S. Xu, and X. Wu, "A review of deep learning in multiscale agricultural sensing," *Remote Sens.*, vol. 14, no. 3, Feb. 2022, Art. no. 559, doi: 10.3390/rs14030559.
[36] Z. Feng et al., "Dynamic cosine method for normalizing incidence angle effect on C-band radar backscattering coefficient for maize canopies based on NDVI," *Remote Sens. (Basel)*, vol. 13, no. 15, Jul. 2021, Art. no. 2856, doi: 10.3390/rs13152856.
[37] M. Belgiu and L. Drăguţ, "Random forest in remote sensing: A review of applications and future directions," *ISPRS J. Photogrammetry Remote Sens.*, vol. 114, pp. 24–31, Apr. 2016, doi: 10.1016/j.isprsjprs.2016.01.011.
[38] S. Wang, G. Azzari, and D. B. Lobell, "Crop type mapping without field-level labels: Random forest transfer and unsupervised clustering techniques," *Remote Sens. Environ.*, vol. 222, pp. 303–317, Mar. 2019, doi: 10.1016/j.rse.2018.12.026.
[39] F. Karim, S. Majumdar, H. Darabi, and S. Harford, "Multivariate LSTM-FCNs for time series classification," *Neural Netw.*, vol. 116, pp. 237–245, Aug. 2019, doi: 10.1016/j.neunet.2019.04.014.
[40] H. Ismail Fawaz et al., "InceptionTime: Finding AlexNet for time series classification," *Data Mining Knowl. Discov.*, vol. 34, no. 6, pp. 1936–1962, Nov. 2020, doi: 10.1007/s10618-020-00710-y.
[41] S. Ahmed and M. Al-Doori, "A study of the importance of sowing dates and plant density affecting some rapeseed cultivars (*Brassica napus L.*)," *College Basic Educ. Res. J.*, vol. 11, pp. 615–632, Mar. 2012.
[42] Z. Xie et al., "Modelling winter rapeseed (Brassica napus L.) growth and yield under different sowing dates and densities using AquaCrop model," *Agronomy*, vol. 13, no. 2, Jan. 2023, Art. no. 367, doi: 10.3390/agronomy13020367.
[43] United States Department of Agriculture, "USDA Rapeseed maps," *USDA Crop Explorer* . Accessed: Feb. 2023. [Online]. Available: https://ipad.fas.usda.gov/cropexplorer/cropview/Default.aspx
[44] D. C. Duro, S. E. Franklin, and M. G. Dubé, "Multi-scale object-based image analysis and feature selection of multi-sensor earth observation imagery using random forests," *Int. J. Remote Sens.*, vol. 33, no. 14, pp. 4502–4526, Jul. 2012, doi: 10.1080/01431161.2011.649864.
[45] E. Ndikumana, D. Ho Tong Minh, N. Baghdadi, D. Courault, and L. Hossard, "Deep recurrent neural network for agricultural classification using multitemporal SAR Sentinel-1 for Camargue, France," *Remote Sens. (Basel)*, vol. 10, no. 8, Aug. 2018, Art. no. 1217, doi: 10.3390/rs10081217.
[46] D. Peng, Y. Zhang, and H. Guan, "End-to-end change detection for high resolution satellite images using improved UNet++," *Remote Sens. (Basel)*, vol. 11, no. 11, Jun. 2019, Art. no. 1382, doi: 10.3390/rs11111382.
[47] D. Chicco, M. J. Warrens, and G. Jurman, "The matthews correlation coefficient (MCC) is more informative than Cohen's Kappa and brier score in binary classification assessment," *IEEE Access*, vol. 9, pp. 78368–78381, 2021.
[48] J. Chang, M. C. Hansen, K. Pittman, M. Carroll, and C. DiMiceli, "Corn and soybean mapping in the United States using MODIS time-series data sets," *Agronomy J.*, vol. 99, no. 6, pp. 1654–1664, Nov. 2007, doi: 10.2134/agronj2007.0170.
[49] L. Pádua, T. Adão, A. Sousa, E. Peres, and J. J. Sousa, "Individual grapevine analysis in a multi-temporal context using UAV-based multi-sensor imagery," *Remote Sens. (Basel)*, vol. 12, no. 1, Jan. 2020, Art. no. 139, doi: 10.3390/rs12010139.
[50] S. Han, J. Liu, G. Zhou, Y. Jin, M. Zhang, and S. Xu, "InceptionV3-LSTM: A deep learning net for the intelligent prediction of rapeseed harvest time," *Agronomy*, vol. 12, no. 12, Dec. 2022, Art. no. 3046, doi: 10.3390/agronomy12123046.
[51] H. Bazzi, N. Baghdadi, M. El Hajj, and M. Zribi, "Potential of sentinel-1 surface soil moisture product for detecting heavy rainfall in the South of France," *Sensors*, vol. 19, no. 4, Feb. 2019, Art. no. 802, doi: 10.3390/s19040802.
[52] A. Mercier et al., "Evaluation of Sentinel-1 and 2 time series for land cover classification of forest–agriculture mosaics in temperate and tropical landscapes," *Remote Sens. (Basel)*, vol. 11, no. 8, Apr. 2019, Art. no. 979, doi: 10.3390/rs11080979.
[53] E. Woźniak et al., "Multi-temporal phenological indices derived from time series Sentinel-1 images to country-wide crop classification," *Int. J. Appl. Earth Observation Geoinf.*, vol. 107, Mar. 2022, Art. no. 102683, doi: 10.1016/j.jag.2022.102683.
[54] G. Waldhoff, U. Lussem, and G. Bareth, "Multi-data approach for remote sensing-based regional crop rotation mapping: A case study for the Rur catchment, Germany," *Int. J. Appl. Earth Observation Geoinf.*, vol. 61, pp. 55–69, Sep. 2017, doi: 10.1016/j.jag.2017.04.009.
[55] G. Bareth, "Multi-data approach (MDA) for enhanced land use/land cover mapping," *Int. Arch. Photogrammetry, Remote Sens. Spatial Inf. Sci.*, vol. 2, no. 10, pp. 1059–1066, 2008.
[56] C. Lin, L. Zhong, X.-P. Song, J. Dong, D. B. Lobell, and Z. Jin, "Early- and in-season crop type mapping without current-year ground truth: Generating labels from historical information via a topology-based approach," *Remote Sens. Environ.*, vol. 274, Jun. 2022, Art. no. 112994, doi: 10.1016/j.rse.2022.112994.
[57] W. Cai, J. Tian, X. Li, L. Zhu, and B. Chen, "A new multiple phenological spectral feature for mapping winter wheat," *Remote Sens. (Basel)*, vol. 14, no. 18, Sep. 2022, Art. no. 4529, doi: 10.3390/rs14184529.
[58] D. M. Johnson and R. Mueller, "Pre- and within-season crop type classification trained with archival land cover information," *Remote Sens. Environ.*, vol. 264, Oct. 2021, Art. no. 112576, doi: 10.1016/j.rse.2021.112576.
[59] N. You and J. Dong, "Examining earliest identifiable timing of crops using all available sentinel 1/2 imagery and Google Earth Engine," *ISPRS J. Photogrammetry Remote Sens.*, vol. 161, pp. 109–123, Mar. 2020, doi: 10.1016/j.isprsjprs.2020.01.001.
[60] R. Yaramasu, V. Bandaru, and K. Pnvr, "Pre-season crop type mapping using deep neural networks," *Comput. Electron. Agriculture*, vol. 176, Sep. 2020, Art. no. 105664, doi: 10.1016/j.compag.2020.105664.
[61] J. L. Hatfield, J. H. Prueger, T. J. Sauer, C. Dold, P. O'Brien, and K. Wacha, "Applications of vegetative indices from remote sensing to agriculture: Past and future," *Inventions*, vol. 4, no. 4, Dec. 2019, Art. no. 71, doi: 10.3390/inventions4040071.

Saeideh Maleki received the Ph.D. degree in environmental planning from the Isfahan University of Technology, Isfahan, Iran, in 2018.

She is currently working as a Researcher with INRAE UMR-TETIS, Montpellier, France. Since 2018, she is also an Assistant Professor with Zabol University, Zabol, Iran. Her main research interests include land surface monitoring using Earth observation data, including optical and microwave remote sensing, and ecosystem change detection. Since 2013, she has been working on various applications of remote sensing, focusing on image processing, remote sensing data analysis applied to land use, land cover detection, and ecosystem studies.

Nicolas Baghdadi received the Ph.D. degree in estimation of coastal currents using remote sensing from the University of Toulon, La Valette-du-Va, France, in 1994.

From 1995 to 1997, he was a Postdoctoral Researcher with INRS Ete – Water Earth Environment Research Centre, Quebec University, Canada. From 1998 to 2008, he was with the French Geological Survey (BRGM), Orleans, France. Since 2008, he has been a Research Director with the French Research Institute of Science and Technology for Environment and Agriculture (IRSTEA, now INRAE). He is the editor of two series of books: *Land Surface Remote Sensing Set* and *QGIS in Remote Sensing Set* http://www.iste.co.uk/subject.php?id = NJNK. His research interests include the analysis of remote sensing data (mainly radar and lidar) and the retrieval of environmental parameters (e.g., soil moisture content, soil roughness, canopy height, forest biomass, etc.). From 2013 to 2022, he was the Scientific Director of the French Land Data Center.

Cassio Fraga Dantas received the Ph.D. degree in signal, image and vision from Inria, Rennes, France, in 2019.

He is a Research Scientist at INRAE, TETIS, Montpellier, France. Between 2020 and 2022, he was a Postdoctoral Researcher with IRIT (computer science laboratory of Toulouse) and IMAG (mathematics laboratory of the University of Montpellier). His current research interests include interpretable artificial intelligence, optimization algorithms and machine learning for remote sensing data with applications to agriculture, ecosystems, and environment.

Sami Najem received the bachelor's degree in biology from Lebanese University, Fanar, Lebanon, in 2017, and the master's degree in biodiversity: management and conservation of natural resources from the Lebanese University, Beirut, Lebanon, in 2019. His master's thesis was centered around drought monitoring in the MENA region using micro-wave remote sensing data.

He is currently a Research Engineer with INRAE UMR-TETIS, Montpellier, France. His research interests include radar and optical remote sensing in the field of agricultural management.

Hassan Bazzi received the Ph.D. degree in remote sensing from AgroParisTech University, Montpellier, France, in 2021.

He is a Data Scientist at Atos France since 2022 and is part of the Atos Inno'Lab (Île-de-France). He is currently a scientific project Manager in an integrated team between Atos and the Laboratory of Climate and Environmental Science (LSCE) of the University of Paris-Saclay, Gif-sur-Yvette, France. His research interests include land surface monitoring using Earth observation data, including optical and microwave remote sensing. Since 2017, he has been working on various applications of remote sensing, focusing on image processing, remote sensing data analysis, and the development of machine learning-based methods applied to hydrology, agronomy, and most recently greenhouse gas modeling.

Núria Pantaleoni Reluy received the graduate degree in geology and environmental sciences from the Universiat Autonoma de Barcelona, Barcelona, Spain, in 2018, and the master's degree in water and agriculture from the Supagro University, Montpellier, France, in 2021.

Currently, curious about the analysis of the vegetative cycle of crops and aware of the stakes and increasing tensions on water resources, she is working in the use of satellite data to monitor the vegetative state of agricultural plots, as well as the study of soil moisture and possible irrigation periods as a INRAE Research Engineer at UMR-TETIS, Montpellier.

Dino Ienco received the M.Sc. and Ph.D. degrees in computer science both from the University of Torino, Torino, Italy, in 2006 and 2010, respectively.

He joined the TETIS Laboratory, IRSTEA, Montpellier, France, in 2011, as a Junior Researcher. His main research interests include machine learning, data science, graph databases, social media analysis, information retrieval and spatio-temporal data analysis with a particular emphasis on remote sensing data and Earth Observation data fusion.

Dr. Ienco served in the program committee of many international conferences on data mining, machine learning, and database including IEEE ICDM, ECML PKDD, ACML, IJCAI as well as served as a Reviewer for many international journal in the general field of data science and remote sensing.

Mehrez Zribi received the B.E. degree in signal processing from the Ecole Nationale Supérieure d'Ingénieurs en Constructions Aéronautiques, Toulouse, France, and the Ph.D. degree in characterization of soil parameters using remote sensing from the Université Paul Sabatier, Toulouse, in 1996.

In 1995, he joined the Centre d'Etude des Environnements Terrestre et Planétaires Laboratory/Institut Pierre Simon Laplace, Vélizy, France. Since October 2008, he has been with the Centre d'Etudes Spatiales de la Biosphère (CESBIO), Toulouse. He is a Research Director with the Centre National de Recherche Scientifique, Toulouse. His research interests include microwave remote sensing applied to hydrology, microwave modeling for land surface parameters estimations and finally airborne microwave instrumentation. He has published more than 150 articles in refereed journals. He is currently the Director of CESBIO.